Using constellation pharmacology to define comprehensively a somatosensory neuronal subclass

Russell W. Teichert[1], Tosifa Memon, Joseph W. Aman, and Baldomero M. Olivera[1]

Department of Biology, University of Utah, Salt Lake City, UT 84112

Contributed by Baldomero M. Olivera, December 30, 2013 (sent for review December 1, 2013)

Change is intrinsic to nervous systems; change is required for learning and conditioning and occurs with disease progression, normal development, and aging. To better understand mammalian nervous systems and effectively treat nervous-system disorders, it is essential to track changes in relevant individual neurons. A critical challenge is to identify and characterize the specific cell types involved and the molecular-level changes that occur in each. Using an experimental strategy called constellation pharmacology, we demonstrate that we can define a specific somatosensory neuronal subclass, cold thermosensors, across different species and track changes in these neurons as a function of development. Cold thermosensors are uniformly responsive to menthol and innocuous cool temperature (17 °C), indicating that they express TRPM8 channels. A subset of cold thermosensors expressed α7 nicotinic acetylcholine receptors (nAChRs) but not other nAChR subtypes. Differences in temperature threshold of cold thermosensors correlated with functional expression of voltage-gated K channels K_V1.1/1.2: Relatively higher expression of K_V1.1/1.2 channels resulted in a higher threshold response to cold temperature. Other signaling components varied during development and between species. In cold thermosensors of neonatal mice and rats, ATP receptors were functionally expressed, but the expression disappeared with development. This developmental change occurred earlier in low-threshold than high-threshold cold thermosensors. Most rat cold thermosensors expressed TRPA1 channels, whereas mouse cold thermosensors did not. The broad implications of this study are that it is now feasible to track changes in receptor and ion-channel expression in individual neuronal subclasses as a function of development, learning, disease, or aging.

DRG | trigeminal | calcium imaging | purinergic receptor | K_V1.2

The rapid advances in genomics and molecular genetics are generating new molecular data at a pace that far exceeds the rate at which the accumulating information can be integrated into higher levels of biological organization. We recently used a combination pharmacology strategy to investigate how multiple molecular targets, as an ensemble, can be used to characterize and functionally define different individual neuronal subclasses. We call this experimental strategy "constellation pharmacology" because we pharmacologically target the integrated combination, or constellation, of receptors and ion channels expressed in specific types of neurons to identify and differentiate between subclasses (1).

As a strategy for identifying a specific neuronal subclass unambiguously and investigating its function, there has been considerable excitement about recent advancements in optogenetics. Through optogenetics, it is possible to activate or inhibit the activity of a specific neuronal subclass, while monitoring the effect on a circuit, network, or behavioral phenotype (2–5). Constellation pharmacology is a complementary approach that also may be used to activate or inhibit the activity of a targeted neuronal subclass. Additionally, it has the potential to provide an unbiased evaluation of neuronal subclasses that is broadly applicable across both model and nonmodel organisms.

In this study, we used constellation pharmacology to identify and characterize molecular changes that occur in one somatosensory neuronal subclass as a function of development. We have compared the results obtained with a model genetic organism (mouse) to a nonmodel organism (rat). Specifically, cold thermosensors from mouse and rat dorsal root ganglia (DRG) and trigeminal ganglia (TG) from neonatal through mature animals were characterized and compared. This study further uncovers the range of variation in cold thermosensors (e.g., low vs. high threshold), also revealing their invariant core and variable ancillary signaling components.

Results

Functional Fingerprints. Here we demonstrate an experimental strategy to identify and functionally characterize neuronal and glial subclasses. The general strategy is to subject a heterogeneous population of >100 cells to a series of diverse pharmacological perturbations, while simultaneously monitoring responses of individual cells by calcium imaging. Using this approach, we can identify different cellular-response phenotypes that we call "functional fingerprints." Each fingerprint corresponds to the cell-specific combination of receptors and ion channels expressed in a particular cellular subclass. Fig. 1 shows selected calcium-imaging traces (i.e., functional fingerprints) of dissociated neuronal and nonneuronal cells from mouse DRG. In this trial, >200 cells were monitored simultaneously, and the responses of 20 of them are illustrated, with each trace representing the response of an individual cell. Most of the functional fingerprints shown in Fig. 1 were observed in multiple cells in this experimental trial, suggesting that each fingerprint represents a particular neuronal or nonneuronal cell type. Fig. 1 shows only one trace of any functional fingerprint to illustrate a subset of the cellular diversity present in a DRG cell population. The diversity of functional fingerprints shows that this experimental methodology can effectively demarcate different neuronal and nonneuronal cell types simultaneously in a single experimental trial. Here we focus on an infrequent neuronal subclass (with

Significance

Change in the nervous system occurs in response to diverse inputs, both normal and pathological. Defining such changes is required for understanding normal nervous-system functions and pathologies—e.g., from learning and memory to intractable disease. A unique combination pharmacology strategy allows identification of distinct neuronal subclasses through their constant functional expression of a specific subset of signaling proteins. Phenotypic alterations in signaling for one specific neuronal subclass were tracked as a function of development. These alterations provide proof-of-principle that changes in individual types of neurons can be monitored as a function of learning, disease, or aging. Developing biomarkers and therapeutic interventions for intractable nervous-system pathologies will require simultaneously monitoring different neuronal subclasses for such changes early during disease progression.

Author contributions: R.W.T. and B.M.O. designed research; R.W.T., T.M., and J.W.A. performed research; R.W.T. and T.M. analyzed data; and R.W.T. and B.M.O. wrote the paper.

The authors declare no conflict of interest.

[1]To whom correspondence may be addressed. E-mail: olivera@biology.utah.edu or russ.teichert@utah.edu.

This article contains supporting information online at www.pnas.org/lookup/suppl/doi:10.1073/pnas.1324019111/-/DCSupplemental.

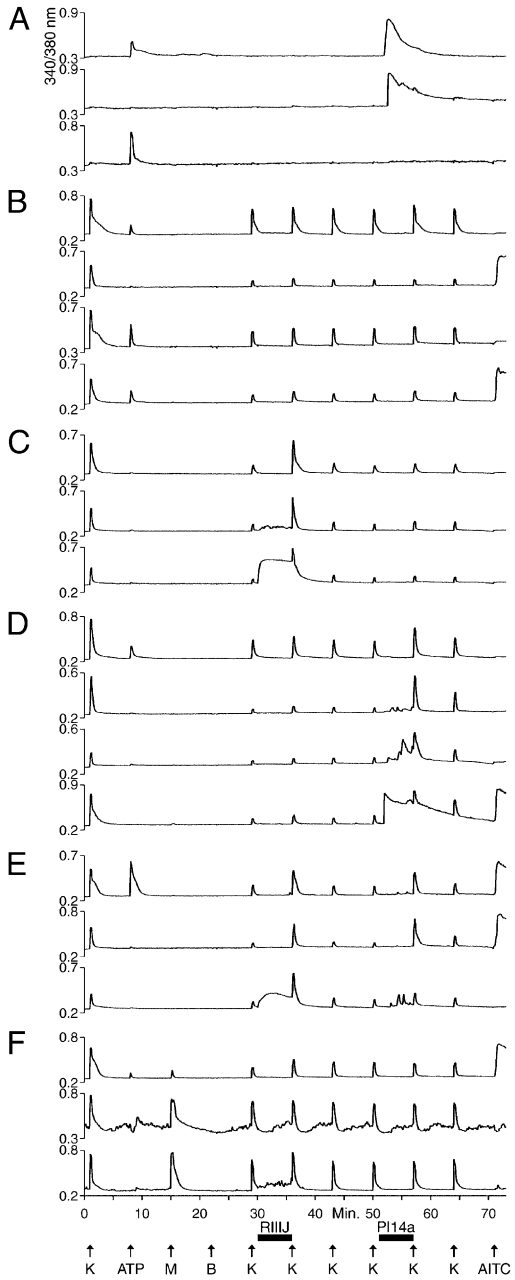

Fig. 1. Selected calcium-imaging traces (functional fingerprints) of individual cells from a mouse DRG cell population. See *Materials and Methods* for a description of the experimental protocol. Each trace is the response of an individual cell from a single experimental trial. At minute 1, K means 30 mM $[K^+]_o$; at all other time points, K means 20 mM $[K^+]_o$. (*A*) Traces from three cells that did not respond to depolarization by 30 mM $[K^+]_o$, indicating that they are not neurons. Two of the cells responded to application of 20 μM ATP, and two responded transiently to application of a cone-snail venom peptide, PI14a (16 μM), a selective antagonist of the voltage-gated K channel, $K_V1.6$. These cells did not respond to application of 1 μM κM–conotoxin RIIIJ (RIIIJ), a selective blocker of $K_V1.2$. (*B*) Traces from neurons that were relatively insensitive to either RIIIJ or PI14a. Two cells responded to ATP, but not 100 μM AITC. One cell responded to AITC, but not ATP. One cell responded to ATP and AITC. (*C*) Three neurons that responded to RIIIJ with a direct response and/or amplification of the response elicited by depolarization with 20 mM $[K^+]_o$. (*D*) Four neurons that responded to PI14a with a direct response and/or amplification of the response elicited by depolarization by 20 mM $[K^+]_o$. Notably, one cell responded to ATP, and one cell responded to AITC. (*E*) Three neurons that responded to both RIIIJ and PI14a, either with direct responses or with amplifications of the responses elicited by depolarization by 20 mM $[K^+]_o$. One cell responded to ATP and AITC. One cell responded to AITC but not ATP. (*F*) Three neurons that responded to 400 μM menthol.

variant forms) that is responsive to both menthol and innocuous cool temperatures. These neurons have the functional fingerprints corresponding to the bottom two traces in Fig. 1*F*. This neuronal subclass represented <5% of the neurons in this mouse DRG cell population and much less than 5% of the total neuronal and nonneuronal cells.

Allyl Isothiocyanate Sensitivity of Cold Thermosensors Across Species. Fig. 2*A* (lower trace) exemplifies a putative cold nociceptor previously characterized from mouse DRG (1). This neuronal subclass was defined by its responsiveness to ATP, menthol, mustard oil [allyl isothiocyanate (AITC)], and noxious cold temperatures (e.g., 5 °C) and by its lack of response to innocuous cool temperatures (e.g., 17 °C). The putative physiological role of such DRG neurons is to transmit signals reporting painfully cold temperatures. Fig. 2*A* (upper trace) shows a neuron that did not respond to menthol or cold (typical of most neurons in these cultures) but that did respond to depolarization by high extracellular potassium concentration, $[K^+]_o$. Such neurons served as controls in the following experiments.

Fig. 2*B* shows examples of the cold thermosensors that are the focus of this work. We previously characterized these neurons from postnatal day (P)45–55 mouse DRG (1), where they were defined by responsiveness to menthol and innocuous cool temperatures—e.g., 17 °C (also responding to colder temperatures)—and by lack of responses to ATP and AITC. The putative physiological role of these neurons is to transmit signals reporting cold-temperature gradients without pain. These neurons were further defined by a transient decrease, or dip, in cytoplasmic calcium concentration, $[Ca^{2+}]_i$, produced by the mere exchange of the static-bath solution (Fig. 2*B*). This decrease in $[Ca^{2+}]_i$ contrasts with the stability of $[Ca^{2+}]_i$ observed in the other cells within these cultures (Figs. 1 and 2*A*). We hypothesized that the $[Ca^{2+}]_i$ instability was caused by activity of transient receptor potential cation channel, subfamily M, member 8 (TRPM8) channels at room temperature (typically ∼23 °C in our experiments) (1). The responsiveness of these neurons to menthol suggested that they express TRPM8 channels (6, 7). Furthermore, cold temperature activates TRPM8 channels, with an activation threshold of ∼26 °C (8). Thus, the $[Ca^{2+}]_i$ dip may have been caused by transient warming, preceded and followed by evaporative cooling of the static bath. Transient warming would stochastically inactivate a subset of TRPM8 channels, which are calcium-permeable and active at room temperature, thereby temporarily reducing $[Ca^{2+}]_i$. Indeed, the bath temperature increased on average by 0.6 °C upon replacement of the static-bath solution, followed by gradual evaporative cooling of the same magnitude. Furthermore, Fig. S1 shows that the $[Ca^{2+}]_i$ baseline did not dip when the bath solution was replaced with a precooled solution of the same temperature, thus confirming that the observed dips were caused by slight transient warming, followed by evaporative cooling.

The mouse and rat neurons depicted in Fig. 2*B* are putative orthologs—i.e., homologous cell types in different species that share a common ancestry. Although there are distinct similarities between these neurons, most rat cold thermosensors were responsive to AITC, whereas only a small minority of mouse cold thermosensors responded to AITC (Fig. 2*B*). This difference in AITC sensitivity was consistent across all preparations of mouse and rat neurons: >65% of rat cold thermosensors were AITC-sensitive across DRG and TG neurons of all ages, whereas <5% of mouse cold thermosensors were AITC-sensitive. For each type of cell preparation (rat or mouse, DRG or TG, neonatal or mature), six or more cell cultures were tested, and ≥46 total cold thermosensors were analyzed. Previous reports have shown that 100 μM AITC selectively activated TRPA1 channels (9–13). Therefore, the results reflect a quantitative difference between rat and mouse; namely, most rat cold thermosensors express functional TRPA1 channels, whereas only a small minority of mouse cold thermosensors expresses TRPA1.

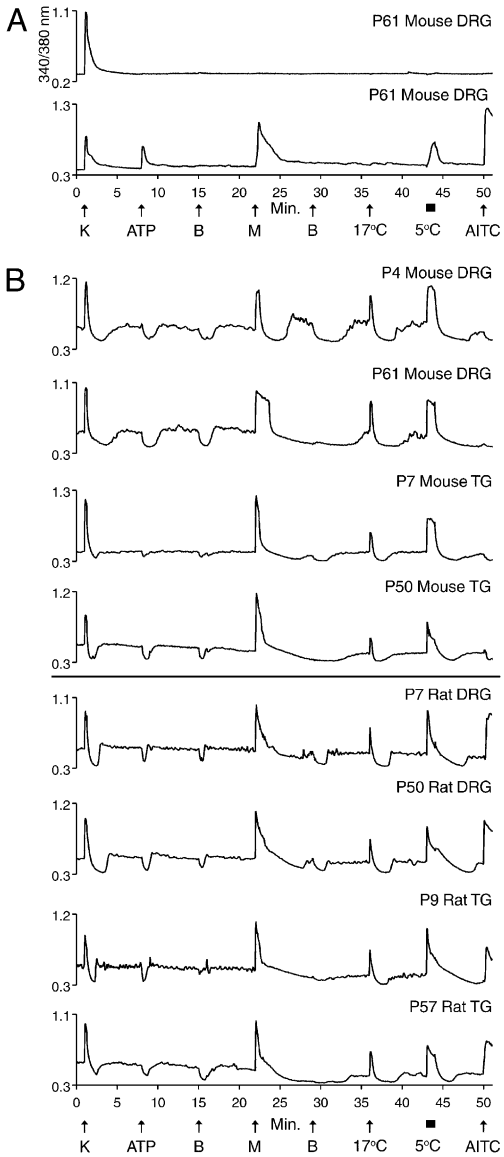

Fig. 2. Species difference in AITC sensitivity of cold thermosensors. See *Materials and Methods* for a description of the experimental protocol. (*A*) (Upper trace) Mouse DRG neuron that only responded to depolarization by 30 mM $[K^+]_o$. (Lower trace) Cold-nociceptor that responded to 20 μM ATP, 400 μM menthol, bath solution at 5 °C, and 100 μM AITC, but not bath solution at 17 °C. (*B*) Cold thermosensors from indicated cultures. Each neuron responded to menthol and bath solution at 17 °C and 5 °C. However, they did not respond to ATP. These neurons exhibited unstable $[Ca^{2+}]_i$ baselines, most evident when bath solution was replaced with identical bath solution (or containing ATP), which caused a transient dip in baseline $[Ca^{2+}]_i$. Neurons from mouse DRG and TG did not respond to AITC (top four traces), whereas those from rat DRG and TG did respond to AITC (bottom four traces).

Low- and High-Threshold Cold Thermosensors During Development. In addition to the cold thermosensors with unstable $[Ca^{2+}]_i$ baselines (Fig. 3*A*), we observed cold thermosensors with stable $[Ca^{2+}]_i$ baselines (Fig. 3*B*). Both cold thermosensors responded to menthol and innocuous cool temperatures (17 °C) and differed only in the stability of baseline $[Ca^{2+}]_i$. As described above, this instability was induced by slight temperature changes when the bath solution was exchanged. Therefore, the cold thermosensors with stable $[Ca^{2+}]_i$ baselines appeared to require colder temperature to observe changes in $[Ca^{2+}]_i$ than the thermosensors with unstable baselines. Additionally, Fig. S1 shows that there is in fact a difference in cold threshold between the thermosensors with unstable and stable baselines. Accordingly, we refer to the variant forms of cold thermosensors as low- and high-threshold cold thermosensors (Fig. 3). Notably, the high-threshold cold thermosensors are intermediate in their cold threshold between low-threshold cold thermosensors with unstable baselines (Fig. 2*B*) and cold nociceptors (Fig. 2*A*), which also have stable baselines. Nevertheless, we will refer to the two variant forms of cold thermosensors as low- and high-threshold, respectively.

We observed a developmental change in low- and high-threshold cold thermosensors. At P4–5, a subset of mouse cold thermosensors was responsive to ATP (Fig. 3), which was also observed in rat cold thermosensors (Fig. S2). At P12–13, no ATP responses were observed in low-threshold cold thermosensors, but a subset of high-threshold cold thermosensors remained ATP-responsive (Fig. 3*C*). By P50, no unambiguous ATP responses were observed in low- or high-threshold cold thermosensors from mouse or rat DRG (Fig. 3*C*), in contrast to ATP responses observed in cold nociceptors from mature mouse DRG (Fig. 2*A*). A qualitative assessment suggested the same developmental change in ATP sensitivity of TG cold thermosensors. Our results are consistent with immunohistochemistry studies showing that nearly all rodent DRG and TG neurons express the $P2X_3$ subtype of ATP-gated ion channels at birth, but in mature animals, the expression is lost in a subset of neurons (14, 15).

Differential Expression of Potassium Channels Between Low- and High-Threshold Cold Thermosensors. Additional differences between low- and high-threshold cold thermosensors were observed in response to blockers of the K_V1 family of voltage-gated K channels, including the following: α-dendrotoxin (α-Dtx), selective for K channels that contain $K_V1.1$, 1.2, or 1.6 subunits (16); dendrotoxin-K (Dtx-K), selective for K channels that contain $K_V1.1$ subunits (17–19); and κM–conotoxin RIIIJ (RIIIJ), selective for K channels that contain $K_V1.2$ subunits (20). Fig. 4*A* demonstrates that low-threshold cold thermosensors were relatively unaffected by these K-channel blockers. However, in some high-threshold cold thermosensors, α-Dtx, Dtx-K, and RIIIJ caused the baseline $[Ca^{2+}]_i$ to increase (Fig. 4*A*). These results suggest that expression of a $K_V1.1/1.2$ heteromer contributes to the higher cold threshold of these neurons.

In Fig. 4*B* (middle trace), we demonstrate that K-channel block by RIIIJ is sufficient to change the phenotype of some high-threshold cold thermosensors into low-threshold cold thermosensors. When the bath solution containing RIIIJ was replaced by identical bath solution, the elevated $[Ca^{2+}]_i$ baseline dipped in a manner similar to the low-threshold cold thermosensors. These effects of RIIIJ on high-threshold cold thermosensors were reversible. Also, RIIIJ had no apparent effect on the low-threshold cold thermosensors (Fig. 4*B*, top trace). Exposure to RIIIJ did not alter the $[Ca^{2+}]_i$ baseline of the cold nociceptors, but did amplify their response to cold temperature (Fig. 4*B*, bottom trace). These differences in sensitivity to RIIIJ are consistent with a report that the threshold of cold-sensitive neurons is determined by a balance between expression levels of TRPM8 and a K_V1 channel (21).

Many high-threshold cold thermosensors were not converted to low-threshold cold thermosensors by RIIIJ, suggesting that there may be other functionally integrated determinants of cold threshold. In addition to TRPM8 and $K_V1.1/1.2$, Ca_V1 calcium channels may play a role in setting the cold threshold. In Fig. 4*C*, a blocker of $K_V1.1/1.2$ (RIIIJ) changed the phenotype of a high-threshold cold thermosensor into that of a low-threshold cold thermosensor (lower trace). In stark contrast to that result, a blocker of Ca_V1 (nicardipine) changed the phenotype of a low-threshold cold thermosensor into that of a high-threshold cold thermosensor (upper trace). Thus, the cold threshold may be set by a complex interaction between differentially expressed ion channels, including TRPM8, $K_V1.1/1.2$, and Ca_V1 channels.

Differential Expression of Nicotinic Acetylcholine Receptors. A final set of experiments to discriminate among cold thermosensors

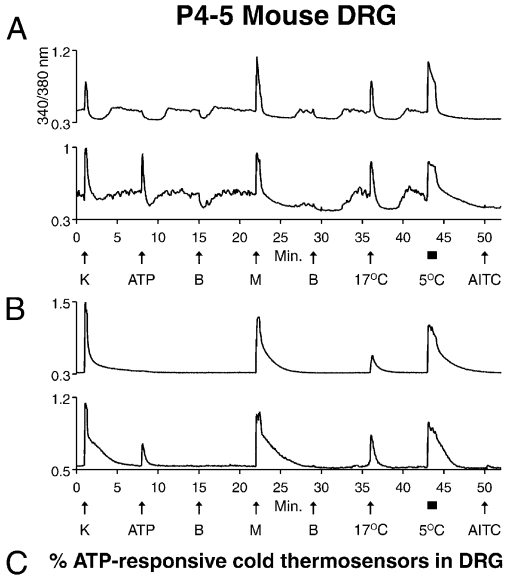

C % ATP-responsive cold thermosensors in DRG

Species	Cold Threshold	P4-5	P12-13	>P50
Mouse	Low	26%	0%	0%
Rat	Low	56%	0%	0%
Mouse	High	83%	53%	0%
Rat	High	89%	55%	0%

Fig. 3. Developmental difference in ATP sensitivity of cold thermosensors. See *Materials and Methods* for a description of the experimental protocol. (*A* and *B*) Traces from P4–5 mouse DRG neurons. (*A*) Low-threshold cold thermosensors, including one that responded to 20 μM ATP (lower trace) and one that did not (upper trace). (*B*) High-threshold cold thermosensors, including one that responded to ATP (lower trace) and one that did not (upper trace). (*C*) A summary of the percentage of ATP-responsive DRG neurons from low- and high-threshold cold thermosensors (exemplified in *A* and *B*) is shown for three different ages of mouse and rat. For each type of cell preparation (rat or mouse at each age), ≥26 cumulative cold thermosensors were examined in five or more independent experimental trials.

demonstrated that many of these neurons functionally express α7 nicotinic acetylcholine (ACh) receptors (nAChRs), but not other nAChR subtypes. As reported by others, there are two subpopulations of DRG neurons with respect to nAChR expression: One subpopulation predominantly expresses homomeric α7 nAChRs, whereas the other subpopulation expresses heteromeric nAChRs containing α3, α6, and β4 subunits (22). We used the positive allosteric modulator of α7 nAChRs, PNU-120596 (PNU), to identify neurons expressing α7 nAChRs. Fig. 5*A* (top trace) is from one of many neurons that responded to ACh with a calcium transient before exposure to PNU. We recently demonstrated that such responses are from heteromeric nAChRs containing α3, α6, and β4 subunits (23), consistent with previous reports. However, many neurons, including the cold thermosensors, responded to ACh only after preincubation with PNU (Fig. 5*A*, middle and bottom traces), which revealed α7 nAChR expression. Presumably, α7 nAChRs desensitize too quickly to produce a detectable calcium transient in the absence of PNU. To confirm that PNU-amplified ACh responses were mediated by α7 nAChRs, we blocked the responses with α-conotoxin ArIB[V11L;V16D], a highly selective antagonist of α7 nAChRs (24) (Fig. 5*B*). Only α7 nAChRs were detected in cold thermosensors across mouse and rat DRG and TG cultures at all ages tested (Fig. S3). Moreover, only a subset of the cold thermosensors exhibited detectable α7 expression in each of these cell populations, which allows cold thermosensors to be further subdivided into variant forms—those that express functional α7 nAChRs and those that do not.

Discussion

Summary of Results. We have provided a comprehensive overview of one neuronal subclass, cold thermosensors, from rat and mouse DRG and TG. The functional fingerprint of cold thermosensors enables us to identify them unequivocally and to compare them across different anatomical loci (lumbar DRG vs. TG) and different rodent species (mouse vs. rat) as a function of development. The results are summarized below and in Table S1. The distinguishing features of cold thermosensors are responsiveness to innocuous cool temperatures (i.e., 17 °C) and to menthol [indicating TRPM8 expression (6, 7)]. These invariant core features stand in contrast to several variable ancillary features. In neonates, most cold thermosensors were ATP-responsive, whereas mature cold thermosensors were not. However, that developmental change occurred earlier for low-threshold than for high-threshold cold

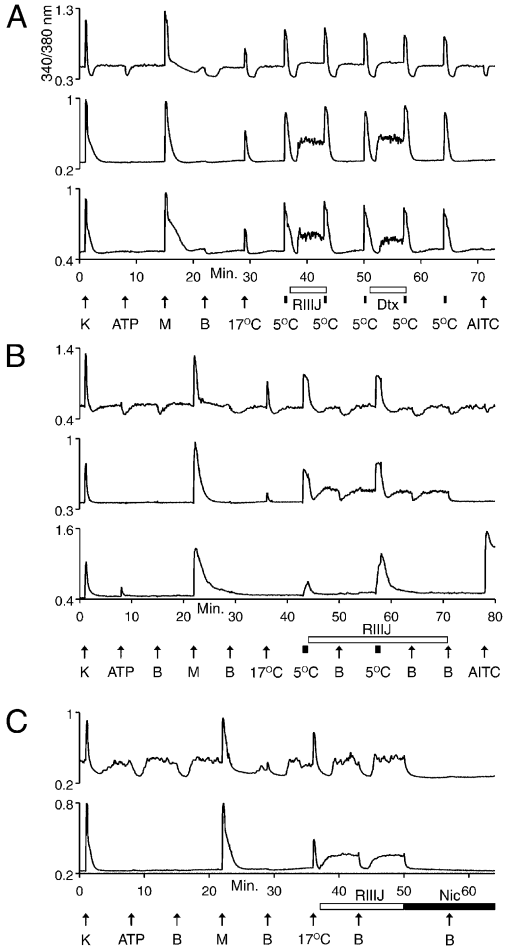

Fig. 4. Cell-type differences in response to K-channel block. See *Materials and Methods* for a description of the experimental protocol. Traces from P11–15 mouse TG neurons. (*A*) (Top trace) Low-threshold cold thermosensor unaffected by 1 μM RIIIJ or 200 nM α-Dtx. (Middle and bottom traces) High-threshold cold thermosensors responded to 1 μM RIIIJ, 200 nM α-Dtx (middle trace), or 200 nM Dtx-K (bottom trace) with increases in $[Ca^{2+}]_i$. (*B*) (Top trace) Low-threshold cold thermosensor unaffected by 1 μM RIIIJ. (Middle trace) Cellular phenotype of high-threshold cold thermosensor changed to low-threshold cold thermosensor by RIIIJ. (Bottom trace) $[Ca^{2+}]_i$ baseline of high-threshold cold-nociceptor was unaltered, but its response to 5 °C was amplified by RIIIJ. (*C*) (Top trace) Low-threshold cold thermosensor unaffected by RIIIJ, but its $[Ca^{2+}]_i$ baseline was blocked to the lowest level observed during $[Ca^{2+}]_i$ dips by 10 μM nicardipine (Nic), and the $[Ca^{2+}]_i$ baseline did not dip in presence of nicardipine upon exchange of bath solution. (Bottom trace) Phenotype of a high-threshold cold thermosensor changed by RIIIJ to that of a low-threshold cold thermosensor.

thermosensors in mouse and rat. Additionally, a subset of cold thermosensors expressed functional α7 nAChRs (but not other nAChR subtypes) in all cell populations tested. Moreover, whereas most cold thermosensors in rat were AITC-responsive, suggesting that they express TRPA1 channels, the large majority of mouse cold thermosensors did not respond to AITC. Finally, relatively higher expression levels of $K_V1.1/1.2$ channels resulted in a higher threshold response to cold temperature. Thus, blocking these channels converted the phenotype of many high-threshold cold thermosensors into low-threshold cold thermosensors.

The difference in sensitivity to RIIIJ between low- and high-threshold cold thermosensors is consistent with a report that the threshold of cold-sensitive neurons is determined by a balance between expression levels of TRPM8 and a K_V1 channel (21). The authors of that study suggested that the K_V1 channel might be a $K_V1.1/1.2$ heteromer, because selective K-channel blockers, including Dtx-K (selective for $K_V1.1$) and TsTx (selective for $K_V1.2$ and 1.3), reduced the cold threshold (21). Our data with RIIIJ (selective for $K_V1.2$), α-Dtx, and Dtx-K support the hypothesis that a $K_V1.1/1.2$ heteromer is involved in setting the cold threshold. In addition to these data, oxaliplatin-induced cold hypersensitivity was associated with down-regulation of $K_V1.1$ expression (25). Furthermore, an endogenous noncoding antisense RNA that suppresses $K_V1.2$ expression has been implicated in hypersensitivity to cold temperature (26, 27). Cumulatively, those data and ours suggest that $K_V1.1/1.2$ heteromers play an important role in cold sensation.

Broad Implications of Results. Our results initiate a systematic functional differentiation of diverse neuronal and glial cell types within the mammalian nervous system, providing a framework for defining the range of variation that occurs in cold thermosensors. The documentation of these variable features allows a concrete basis for investigating specific questions related to the physiological function of cold thermosensors. How does the disappearance of ATP receptors correlate with changes in cold sensation as a function of development? What species difference in cold sensation between mouse and rats may account for the presence of TRPA1 channels in rat, but not mouse, cold thermosensors?

Our results demonstrate that constellation pharmacology is also useful for evaluating the functional integration of molecular components at the cellular level. Although all cold thermosensors observed in our study appear to express TRPM8 channels, they exhibit different thresholds of cold sensitivity. At the molecular level, it is unclear how a single protein (TRPM8 channel) expressed in different cells could produce different temperature thresholds for each cold-sensitive neuron (21). However, our data and those of others (21) suggest that TRPM8 channels are functionally coupled to $K_V1.1/1.2$ channels. Furthermore, our data suggest that the temperature threshold may be set by a complex set of functionally integrated ion channels, potentially including TRPM8, $K_V1.1/1.2$, and Ca_V1 channels. These results can be extrapolated broadly: Functional integration of cell-specific receptors and ion channels produces the unique properties of each neuronal subclass. This functional integration can be studied by constellation pharmacology.

Neuronal Subclasses Identified Through Functional Fingerprints. Using our experimental strategy, we first generated an array of functional fingerprints from a heterogeneous cell population (Fig. 1), using a pharmacological protocol tailored to the neuronal subclasses to be defined. Such fingerprints reveal multiple phenotypic differences, thereby demarcating specific neuronal subclasses. Notably, even narrowly distributed molecular signaling components may be expressed by multiple neuronal subclasses (28). Thus, a combination of subtype-selective pharmacological agents may be required to identify a particular subclass. Here we demonstrated that a functional fingerprint could be sufficiently robust to identify a specific neuronal subclass from different tissues, species, and stages of development. The ability to identify unambiguously a neuronal subclass enables investigators to compare a common set of neurons across studies (29). At present,

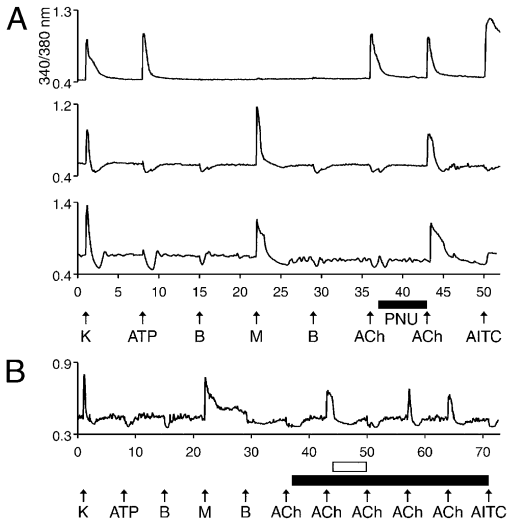

Fig. 5. Cell-type similarity in α7 nAChR responses among a subset of cold thermosensors. See *Materials and Methods* for a description of the experimental protocol. (*A*) (Top trace) Neuron that responded to depolarization by 30 mM $[K^+]_o$, 20 μM ATP, 1 mM ACh, and 100 μM AITC with transient increases in $[Ca^{2+}]_i$. This neuron responded to 1 mM ACh before application of 10 μM PNU. Such neurons served as controls. (Bottom two traces) Low-threshold cold thermosensors responded to ACh only after preincubation with PNU, suggesting that they express α7 nAChRs. The middle trace is from mouse TG, and the bottom trace is from rat DRG. (*B*) The PNU-enhanced, ACh-induced responses were blocked by the selective antagonist of α7 nAChRs, α-conotoxin ArIB[V11L;V16D]. The filled horizontal bar indicates when 10 μM PNU was present, and the open horizontal bar indicates when 200 nM α-conotoxin ArIB [V11L;V16D] was present. No response to 1 mM ACh was observed before PNU application. After preincubation with PNU, this neuron responded to applications of ACh. The responses were blocked reversibly by α-conotoxin ArIB [V11L;V16D].

neuronal subclasses are defined idiosyncratically by each researcher, which impedes accurate comparisons. For example, there is considerable controversy in the scientific literature regarding cold- and menthol-sensitive neurons. Part of this controversy may originate from the investigation of different subsets of cold- and menthol-sensitive neurons by different researchers (e.g., different species, ages, anatomical loci, cold threshold, etc.) (30). Similar confusion and controversy across the peripheral nervous system and CNS has prompted several neuroscientists to call for a standardized classification scheme for neuronal subclasses (29, 31, 32).

By our method, we identified core and ancillary components of specific neuronal subclasses, thus enabling a unifying conceptual framework that could ultimately delineate and standardize cell types. In the same way that cerebellar Purkinje cells are recognized as a distinct neuronal subclass, cold thermosensors could similarly be considered a distinct neuronal subclass, even though these neurons cannot be identified anatomically. We have determined some of the complicating factors in identifying cold thermosensors. For example, cold thermosensors in neonatal rats express TRPA1 channels and ATP receptors, whereas those in adult mice do not. Nevertheless, they are presumably homologous neurons (sharing a common function and embryonic origin). One difference (TRPA1 expression) is due to species divergence, whereas the other (ATP receptor expression) is a function of development. To understand how homologous cells may change from a genetic model organism (e.g., mouse) to non-model organisms (e.g., rats and humans), comparative studies are necessary. Constellation pharmacology enables such comparative studies and, in principle, enables us to track molecular changes in neurons as a function of development, learning, conditioning, disease, injury, or aging.

Optogenetics and Constellation Pharmacology as Complementary and Synergistic Platforms. Optogenetics is viewed as a breakthrough technology that can link molecular-level causes to systems-level effects. As one example, optogenetics can be used to activate or inactivate specific neuronal subclasses, while evaluating the effects on circuits, networks, and behavior (2–5). Using constellation pharmacology, we can evaluate the functional integration of molecular signaling components at the cellular level, which complements the elucidation of functionally integrated cellular components at the systems level by optogenetics. Our results also suggest that optogenetic manipulations at a systems level could be verified by constellation pharmacology, provided that the pharmacological agents are sufficiently selective. Furthermore, results obtained by optogenetics, mostly limited to genetic model organisms, may be extended and compared with nonmodel organisms through the application of constellation pharmacology. Thus, there is considerable potential for a powerful approach that combines optogenetics and constellation pharmacology, thereby bridging different levels of biological organization from molecular through systems neuroscience.

Materials and Methods

All experiments were approved by the Institutional Animal Care and Use Committee of the University of Utah. In all cases, rats were Sprague–Dawley, and mice were C57BL/6. Cell preparation methods and calcium-imaging methods have been described in detail (1, 33). Briefly, following overnight in culture, dissociated cells were loaded with Fura-2-AM dye for 1 h at 37 °C and then 0.5 h at room temperature before ratiometric calcium imaging. Except as indicated, all experiments were performed at room temperature. In experimental trials, individual responses from 100–300 neurons were simultaneously monitored. The following facts apply to all figures: The *x* axis is in minutes, and the *y* axis is the ratio of emission at 510 nm obtained from alternating excitation at 340 and 380 nm, a measure of $[Ca^{2+}]_i$. Each trace represents the response of a single neuron. Upward or downward deflection of a trace indicates an increase or decrease in $[Ca^{2+}]_i$, respectively. Arrows and horizontal bars below the *x* axis represent the time during which a compound or temperature change (from room temperature) was applied to the bath. Each arrow represents a 15-s bath application, and each horizontal bar is on the time scale of the *x* axis. Arrows and bars apply to all traces in a panel (or all panels in the case of Fig. 1). As described in detail (1, 33), after a 15-s bath application of a compound or high extracellular potassium, $[K^+]_o$ (indicated by arrows in figures), the compound or high $[K^+]_o$ was washed out of the bath by replacing the static bath solution with fresh bath solution that did not contain the compound or high $[K^+]_o$. An additional wash (replacement of static bath solution) was performed after 45 s to remove any residual compound from the bath. After applications of menthol, five washes were performed over the same 45-s interval, to wash residual menthol from the bath. In some cases, at the end of an experiment, no washes were performed after AITC was applied. Abbreviations used in multiple figures are: AITC, 100 μM Allyl Isothiocyanate; ATP, 20 μM adenosine 5′-triphosphate; B, bath replacement (i.e., replacement of static bath solution with fresh bath solution); K, 30 mM $[K^+]_o$; M, 400 μM menthol; Pl14a, 16 μM conopeptide Pl14a; PNU, 10 μM PNU-120596; RIIIJ, 1 μM κM-conopeptide RIIIJ; 5 °C or 17 °C refer to replacement of room-temperature bath solution with bath solution at the specified temperature.

ACKNOWLEDGMENTS. We thank My Huynh for assistance in preparing figures. This work was supported by National Institute of General Medical Sciences Grant GM48677.

1. Teichert RW, et al. (2012) Characterization of two neuronal subclasses through constellation pharmacology. *Proc Natl Acad Sci USA* 109(31):12758–12763.
2. Cardin JA, et al. (2010) Targeted optogenetic stimulation and recording of neurons in vivo using cell-type-specific expression of Channelrhodopsin-2. *Nat Protoc* 5(2):247–254.
3. Packer AM, Roska B, Häusser M (2013) Targeting neurons and photons for optogenetics. *Nat Neurosci* 16(7):805–815.
4. Reiner A, Isacoff EY (2013) The Brain Prize 2013: The optogenetics revolution. *Trends Neurosci* 36(10):557–560.
5. Smedemark-Margulies N, Trapani JG (2013) Tools, methods, and applications for optophysiology in neuroscience. *Front Mol Neurosci* 6:18.
6. McKemy DD, Neuhausser WM, Julius D (2002) Identification of a cold receptor reveals a general role for TRP channels in thermosensation. *Nature* 416(6876):52–58.
7. Peier AM, et al. (2002) A TRP channel that senses cold stimuli and menthol. *Cell* 108(5): 705–715.
8. Bautista DM, et al. (2007) The menthol receptor TRPM8 is the principal detector of environmental cold. *Nature* 448(7150):204–208.
9. Bautista DM, et al. (2006) TRPA1 mediates the inflammatory actions of environmental irritants and proalgesic agents. *Cell* 124(6):1269–1282.
10. Jordt SE, et al. (2004) Mustard oils and cannabinoids excite sensory nerve fibres through the TRP channel ANKTM1. *Nature* 427(6971):260–265.
11. Karashima Y, et al. (2007) Bimodal action of menthol on the transient receptor potential channel TRPA1. *J Neurosci* 27(37):9874–9884.
12. Karashima Y, et al. (2009) TRPA1 acts as a cold sensor in vitro and in vivo. *Proc Natl Acad Sci USA* 106(4):1273–1278.
13. Everaerts W, et al. (2011) The capsaicin receptor TRPV1 is a crucial mediator of the noxious effects of mustard oil. *Curr Biol* 21(4):316–321.
14. Chen Y, Li G, Huang LY (2012) P2X7 receptors in satellite glial cells mediate high functional expression of P2X3 receptors in immature dorsal root ganglion neurons. *Mol Pain* 8:9.
15. Ruan HZ, Moules E, Burnstock G (2004) Changes in P2X3 purinoceptors in sensory ganglia of the mouse during embryonic and postnatal development. *Histochem Cell Biol* 122(6):539–551.
16. Harvey AL, et al. (1998) What can toxins tell us for drug discovery? *Toxicon* 36(11): 1635–1640.
17. Robertson B, Owen D, Stow J, Butler C, Newland C (1996) Novel effects of dendrotoxin homologues on subtypes of mammalian Kv1 potassium channels expressed in Xenopus oocytes. *FEBS Lett* 383(1-2):26–30.
18. Sokolov MV, Shamotienko O, Dhochartaigh SN, Sack JT, Dolly JO (2007) Concatemers of brain Kv1 channel alpha subunits that give similar K+ currents yield pharmacologically distinguishable heteromers. *Neuropharmacology* 53(2):272–282.
19. Wang FC, et al. (1999) Identification of residues in dendrotoxin K responsible for its discrimination between neuronal K^+ channels containing Kv1.1 and 1.2 α subunits. *Eur J Biochem* 263(1):222–229.
20. Chen P, Dendorfer A, Finol-Urdaneta RK, Terlau H, Olivera BM (2010) Biochemical characterization of kappaM-RIIIJ, a Kv1.2 channel blocker: Evaluation of cardioprotective effects of kappaM-conotoxins. *J Biol Chem* 285(20):14882–14889.
21. Madrid R, de la Peña E, Donovan-Rodriguez T, Belmonte C, Viana F (2009) Variable threshold of trigeminal cold-thermosensitive neurons is determined by a balance between TRPM8 and Kv1 potassium channels. *J Neurosci* 29(10):3120–3131.
22. Hone AJ, Meyer EL, McIntyre M, McIntosh JM (2012) Nicotinic acetylcholine receptors in dorsal root ganglion neurons include the α6β4* subtype. *FASEB J* 26(2):917–926.
23. Smith NJ, et al. (2013) Comparative functional expression of nAChR subtypes in rodent DRG neurons. *Front Cell Neurosci* 7:225.
24. Whiteaker P, et al. (2007) Discovery, synthesis, and structure activity of a highly selective alpha7 nicotinic acetylcholine receptor antagonist. *Biochemistry* 46(22):6628–6638.
25. Descoeur J, et al. (2011) Oxaliplatin-induced cold hypersensitivity is due to remodelling of ion channel expression in nociceptors. *EMBO Mol Med* 3(5):266–278.
26. Han TW, Jan LY (2013) Making antisense of pain. *Nat Neurosci* 16(8):986–987.
27. Zhao X, et al. (2013) A long noncoding RNA contributes to neuropathic pain by silencing Kcna2 in primary afferent neurons. *Nat Neurosci* 16(8):1024–1031.
28. Nelson SB, Hempel C, Sugino K (2006) Probing the transcriptome of neuronal cell types. *Curr Opin Neurobiol* 16(5):571–576.
29. Nelson SB, Sugino K, Hempel CM (2006) The problem of neuronal cell types: A physiological genomics approach. *Trends Neurosci* 29(6):339–345.
30. McKemy DD (2005) How cold is it? TRPM8 and TRPA1 in the molecular logic of cold sensation. *Mol Pain* 1:16.
31. Bernard A, Sorensen SA, Lein ES (2009) Shifting the paradigm: New approaches for characterizing and classifying neurons. *Curr Opin Neurobiol* 19(5):530–536.
32. Yano K, Subkhankulova T, Livesey FJ, Robinson HP (2006) Electrophysiological and gene expression profiling of neuronal cell types in mammalian neocortex. *J Physiol* 575(Pt 2):361–365.
33. Teichert RW, et al. (2012) Functional profiling of neurons through cellular neuropharmacology. *Proc Natl Acad Sci USA* 109(5):1388–1395.